Research Article | Vol. 58, No. 10 / 1 April 2019 / Applied Optics 2575

applied optics

Application of neutral-density filters to nonuniformity correction

SONGTAO CHANG* AND YAOYU ZHANG

Changchun Institute of Optics, Fine Mechanics and Physics, Chinese Academy of Sciences, Changchun 130033, China
*Corresponding author: stchang2010@sina.com

Received 4 January 2019; revised 26 February 2019; accepted 26 February 2019; posted 27 February 2019 (Doc. ID 356855); published 27 March 2019

Two-point nonuniformity correction (NUC) is the most effective and commonly used algorithm for scientific and commercial infrared imagers. However, conventional two-point NUC requires two references at different levels of flux, which are sometimes difficult to obtain. To overcome this drawback, a neutral-density filter based solution for two-point NUC of cooled infrared focal plane arrays is proposed in this paper. Benefiting from the specially designed filters and an additional concave mirror, NUC can be conducted by using a single reference at ambient temperature. Several experiments were conducted to validate the performance of the proposed NUC method. The results indicate that it yields excellent performance compared with conventional NUC methods; moreover it is more economical and convenient in various applications.

https://doi.org/10.1364/AO.58.002575

1. INTRODUCTION

A conventional infrared imager is composed of an infrared detector and an optical system, supported by other mechanical and electronic components. Infrared focal plane arrays (IRFPAs), consisting of two-dimensional detector arrays, are the most popular infrared detectors nowadays. However, IRFPAs suffer from undesired spatial nonuniformity owing to the nonuniform response of the individual detectors when illuminated by the same level of irradiance [1–3]. A number of papers and patents that address this problem have been published in recent years [1–5]. Nonuniformity correction (NUC) methods fall into two categories, namely calibration-based techniques and scene-based techniques [6]. Calibration-based NUC methods, such as one-point NUC and two-point NUC, have the benefit of providing radiometrically accurate imagery, although at the cost of periodically obstructing camera operation [7]. Scene-based techniques, which exploit only the information in the scenes that are imaged, avoid the disadvantages of calibration-based techniques at the expense of the loss of radiometrical accuracy [4,5]. High-end and scientific infrared imagers are usually required to produce absolutely calibrated images in units of temperature or radiance, rather than just nonuniformity corrected images [8,9]. Radiometric calibration, which is generally performed using images before NUC, is essential to obtain the relationship between the gray levels of detectors and the radiance. Given the NUC coefficients and a corrected image, the gray levels of the uncorrected image (or the image before NUC) can be easily computed. Thereupon, the radiometrical accuracy will not be decreased by NUC as long as the correction coefficients are known. The correction coefficients of scene-based NUC techniques are updated frequently and not saved. Hence they are not applicable in such measuring applications. Two-point calibration-based NUC, at present, is the most effective and commonly used method for NUC especially for high-end cooled infrared detectors [6]. Generally, two-point NUC performs better than one-point NUC and scene-based techniques, whereas several additional devices (blackbody sources, electromechanical parts, etc.) are required to obtain two references at different levels for two-point correction. This naturally increases the complexity and cost of infrared imaging systems. Consequently, two-point NUCs are recommended to conduct once a month or longer by the manufacturer. However, the spatial nonuniformity, including the nonuniformity of the response and the bias, tends to drift slowly and randomly with time. As a result, one-time factory NUC will not provide a permanent solution to NUC of infrared imagers [4]. To solve this problem, two methods without using blackbody for NUC have been employed, namely one-point additional correction and integration-based NUC. They are conducted by using a single scene at ambient temperature rather than a blackbody as a NUC reference. 1) One-point additional correction means a combination of two-point correction and one-point correction. Two-point correction is used as a default setting, and the one-point correction is conducted frequently for updating the offset correction coefficients. Unfortunately, the performance is unsatisfying compared to two-point NUC because the gain coefficient is not modified by one-point additional correction. 2) Integration-based NUC requires a reference at ambient temperature rather than a blackbody, and varies the integration time to obtain "two different levels" becoming a convenient and economical solution. Nonetheless, the performance of integration-based NUC is poor due to the difference in dark current, fixed pattern noise, and pixel responsiveness under various integration times, which results in fringes, speckle pattern, local inhomogeneity, and other defects.

In summary, two-point NUC using a single reference at ambient temperature is an ideal solution for this problem. By the combination of a concave mirror and a neutral-density filter, the incident flux of an infrared detector can be attenuated while introducing extremely low stray radiation. Based on this design, we propose a neutral-density filter based solution for two-point NUC to decrease the cost and complexity of conventional methods. A short outline is presented as follows: in Section 2, the principles and shortcomings of one-point NUC and the neutral-density filter are described. In Section 3, the design method of the neutral-density filter, which can be used to change the incident flux, is proposed. Hence the two-point NUC method can be achieved using a single reference at ambient temperature. Several NUC experiments were performed to verify the theories described above in Section 4. It is concluded in Section 5 that the proposed method improves the convenience of two-point NUC while ensuring good performance.

2. TWO-POINT NUC AND NEUTRAL-DENSITY FILTERS

A. Principle of Two-Point NUC

Infrared systems, in many applications, are operated in a range of irradiance within which detectors exhibit linear input–output characteristics. The output gray value of a single detector is given by the approximate linear relation [10,11]:

$$Y_{i,j}^{(k)} = G_{i,j}^{(k)} \times X^{(k)} + O_{i,j}^{(k)} + \sigma_{i,j}^{(k)}, \tag{1}$$

where k denotes the frame number. $G_{i,j}$ and $O_{i,j}$ are, respectively, the response and bias of the (i,j)th detector, and X denotes the true infrared radiance of the imaging target. $\sigma_{i,j}$ refers to the temporal noise, which can be effectively reduced by averaging 20 or more frames. In general, the responses and biases of pixels are different, and NUC intends to draw them to uniform. After NUC, the calibration formula, Eq. (1), should be theoretically corrected to

$$\overline{Y} = \overline{G} \times X + \overline{O}, \tag{2}$$

where $\bar{Y}$ denotes the average of pixel outputs, $\bar{G}$ is the mean of the responses of all pixels, and $\bar{O}$ is the mean bias. Two-point NUC draws the calibration curves of all pixels to a single line; hence the response and bias are corrected to be uniform, whereas the commonly used one-point NUC brings the offset to be uniform. For a cooled or high-end infrared imaging system, the response of each pixel is linear to the incident radiance. Therefore two-point NUC provides satisfactory performance. To conduct two-point NUC, two reference resources, respectively at low temperature T_l and high temperature T_h, provided by a surface-area blackbody radiator, are essentially required. Suppose the blackbody temperature is set to a low temperature T_l and a high one T_h, respectively. According to the detector response formula Eq. (1), we obtain

$$\begin{cases} Y_{i,j}(T_l) = G_{i,j} \times X_{i,j}^{(k)}(T_l) + O_{i,j}^{(k)} \\ Y_{i,j}(T_h) = G_{i,j} \times X_{i,j}^{(k)}(T_h) + O_{i,j}^{(k)} \end{cases}. \tag{3}$$

The gain and offset correction coefficients of two-point NUC are, respectively, expressed as

$$\begin{cases} \alpha_{i,j} = \frac{\overline{Y}(T_h) - \overline{Y}(T_l)}{Y_{i,j}(T_h) - Y_{i,j}(T_l)} \\ \beta_{i,j} = \overline{Y}(T_h) - \alpha_{i,j} \cdot Y_{i,j}(T_h) \end{cases}. \tag{4}$$

Despite providing radiometrically accurate corrected imagery, two-point NUC requires a blackbody radiator as the reference, which is inconvenient in many applications. Moreover, most commercial infrared systems are not equipped with a blackbody for cost reasons.

B. Neutral-Density Filters

A neutral-density filter is a common component in infrared imaging systems. Its function is to attenuate the incident radiant energy proportionally, thereby increasing the dynamic range of the system. Some infrared systems have several neutral-density filters that can be switched. For example, four filters with 100%, 50%, 20%, and 10% transmittance, respectively, are used in an infrared telescope. The filters can be automatically switched by a linear motor to attenuate the incident flux proportionately as desired. A cooled infrared detector with a neutral-density filter is shown in Fig. 1. The neutral-density filter is mounted near the Dewar window, or the cold shield.

Cooled short-wave infrared detectors are typically cooled to about 200 K (−73°C) by semiconductor refrigeration technology. Since mid-wave and long-wave infrared detectors are more sensitive to thermal energy, liquid nitrogen refrigeration or Stirling refrigeration is used to cool the detectors to about 77 K (−196°C). According to the law of blackbody radiation, the radiances at 200 K and 77 K are negligible compared to that of ambient temperature, for example, 25°C. By inserting a neutral-density filter, two kinds of stray radiation will be introduced: one is the radiation of the filter itself, determined by the temperature and emissivity; the other is the ambient radiation reflected by the filter and subsequently reaches the IRFPA. The neutral-density filters are classified into absorption-type and reflection-type ones according to the characteristics of the surface coating. For an absorption-type filter, such as a 50% attenuated filter, the absorbance is close to 50% and the emissivity is equal to the absorptivity, while the reflectivity can be ignored.

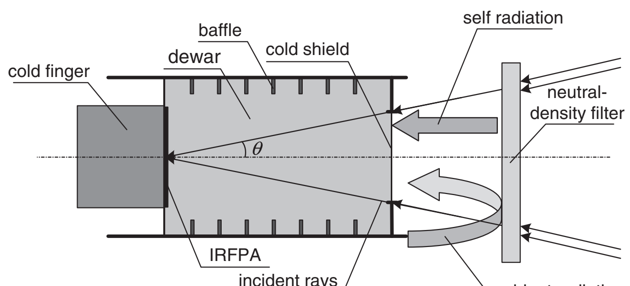

Fig. 1. Effect of a neutral-density filter on IRFPA.

The neutral-density filters are typically not cooled; in other words, their temperatures are close to ambient. Therefore, stray radiation introduced by the absorption-type filter is considerable. It is roughly estimated that if the incident radiance is close to the ambient radiance, the absorption-type filter would not reduce the energy that reaches the detector, as if the filter does not exist. For a reflection-type filter with 50% attenuation, the emissivity is negligible, while the reflectivity reaches almost 50%. According to modeling and calculation, the reflection-type filter introduces stray radiation slightly less than that of the absorption-type filter. To make matters worse, the reflected ambient radiation reaching the detector is not uniform, which is unfavorable to infrared imaging, radiometric calibration, and NUC.

In summary, the neutral-density filters introduce a considerable amount of stray radiation. As a result, the incident radiation of a reference at ambient temperature cannot be effectively attenuated by a neutral-density filter. Besides, the stray radiation caused by the filter might not be uniform.

3. NEUTRAL-DENSITY FILTER BASED NUC METHOD

Two-point NUC can be achieved by using a single reference at ambient temperature with the aid of specially designed neutral-density filters in this paper. The incident radiation emitted by the ambient-temperature reference, namely a "high-temperature reference," can be attenuated by a filter to obtain a "low-temperature reference." Hence two points are obtained for NUC. The key of this two-point NUC solution is to eliminate the stray radiation introduced by the filter, so that the filter can effectively attenuate the incident radiant energy and does not affect the uniformity of the energy received by the detector. In this section, a combination of a concave mirror and a reflective filter is designed to achieve the functions described above.

A. Design of the Concave Mirror

The fundamental principle of the concave mirror is to block the incident flux towards the infrared detector while introducing extraordinarily low stray radiation. In detail, the introduced radiation of a concave mirror can be classified into two categories, namely the reflected ambient radiation and the radiation emitted by the mirror itself. To decrease the latter radiation, the reflecting surface of the concave mirror is polished and coated with high-reflection film, which has extraordinarily low emissivity. The reflected ambient radiation can be eliminated by blocking the path that the ambient radiation reaches the detector. In other words, the detector cannot "see" the ambient out of the field of view. According to the reversibility principle of the ray path, all the rays traced from the infrared detector are completely reflected back to the cryogenic Dewar by a concave mirror. According to ray tracing and analysis, the reflector can be spherical, parabolic, or in other shapes. Since a spherical surface is favorable for analysis, designing, and machining, we designed spherical concave mirrors in this paper.

The shape design principle of the concave mirror is demonstrated in Fig. 2. By appropriate design of the surface curvature, outline diameter, and installation site, ambient radiation outside the cold shield is unable to reach the detector directly.

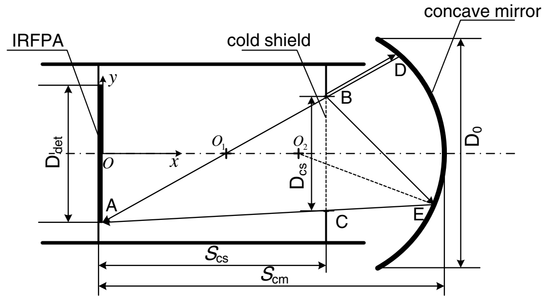

Fig. 2. Principle of the concave mirror.

Moreover, the emissivity of the spherical surface is extraordinarily low, so the stray radiation introduced by the concave mirror is effectively controlled.

As shown in Fig. 2, D_{det} is the diagonal length of the detector, D_{cs} is diameter of the cold shield, S_{cs} is the distance between the cold shield and the detector, and S_{cm} denotes the distance between the concave mirror's vertex and the detector. With the detector center as origin o, a Cartesian coordinate system is established. Axis ox points from the detector to the concave mirror. Given the center of the spherical mirror $(x_c, 0)$, the radius of the reflecting surface can be expressed as $R = S_{cm} - x_c$. The cross section of the spherical reflecting surface is a portion of a circular arc, and the quadratic equation of the circle is given by

$$[x - (S_{cm} - R)]^2 + y^2 = R^2. \quad (5)$$

The radius of the sphere is within a certain range to ensure that the external radiation cannot reach the detector by reflecting. For simplicity, several critical rays are selected to determine the acceptable range of the spherical radius. The IRFPA is in shape of a rectangle. Hence it obtains no incident flux as long as the rays emitted from four corners cannot reach the thermal environment background. Since the infrared optical system is rotationally symmetric and the detector is axisymmetric, only one vertex A of the detector is required to be considered while analyzing. According to the principle of spherical reflection and the analysis of geometric relations between the concave mirror and the detector, it is found that if the ray in direction AB is reflected by point D to point B (edge of the cold shield), the radius of the reflecting spherical surface corresponds to the maximum one, namely R_{max}. The coordinates of point A and B are, respectively, $(0, -D_{det}/2)$ and $(S_{cs}, D_{cs}/2)$; thereupon the equation of line AB can be represented in the form of a straight-line equation as

$$y = k_1 \cdot x + b_1, \quad (6)$$

where $k_1 = (D_{cs} + D_{det})/2S_{cs}$ and $b_1 = -D_{det}/2$.

According to the law of spherical reflection, the intersection of line AB and the axis ox coincides with the spherical center. Therefore the maximum radius of the spherical reflecting surface is

$$R_{max} = S_{cm} - \frac{D_{det}}{D_{cs} + D_{det}} \cdot S_{cs}. \quad (7)$$

Additionally, the critical ray AC originates from the positive edge of the detector diagonal line and passes though the edge of the cold shield. It strikes at E on the reflecting surface, and afterwards goes through the edge of the cold shield. Infrared rays emitted by the external thermal background travel along path BECA to the detector, whereby the path determines the minimum radius $R_{\min}$ of the reflecting sphere. The coordinate of point C is $(S_{cs}, -D_{cs}/2)$, such that the equation of line AC is given by

$$y = (-D_{cs} + D_{det})/2S_{cs} \cdot x - D_{det}/2. \tag{8}$$

For simplicity, Eq. (8) can be written as

$$y = k_2 \cdot x + b_2, \tag{9}$$

where $k_2 = (-D_{cs} + D_{det})/2S_{cs}$ and $b_2 = -D_{det}/2$. Submitting Eq. (5) to Eq. (8) yields the coordinate of point E, which is expressed as $(x_E(R_{\min}), y_E(R_{\min}))$. Thereupon, the formula of line BE is given by

$$y = \frac{y_E(R_{\min}) - D_{cs}/2}{x_E(R_{\min}) - S_{cs}} \cdot (x - S_{cs}) + D_{cs}/2. \tag{10}$$

For simplicity, Eq. (10) can be written as

$$y = k_3 \cdot x + b_3, \tag{11}$$

where $k_3 = \frac{y_E(R_{\min}) - D_{cs}/2}{x_E(R_{\min}) - S_{cs}}$ and $b_3 = D_{cs}/2 - S_{cs} \cdot k_3$.

Assuming that the coordinate of the sphere center is $O_2(x_c, 0)$, then line O_2E is the angular bisector of $\angle$AEB. According to the properties of the angular bisector, the distance between point O_2 and line AC is equal to the distance between O_2 and line BE, such that

$$\frac{|k_2 \cdot (S_{cm} - R_{\min}) + b_2|}{\sqrt{k_2^2 + 1}} = \frac{|k_3 \cdot (S_{cm} - R_{\min}) + b_3|}{\sqrt{k_3^2 + 1}}. \tag{12}$$

The coordinate of point E, namely $(x_E(R_{\min}), y_E(R_{\min}))$, can be determined by Eqs. (5) and (8). By submitting $(x_E(R_{\min}), y_E(R_{\min}))$ to Eqs. (8)–(12), we can obtain $R_{\min}$. The curvature radius of the concave mirror is in the range of $R \in [R_{\min}, R_{\max}]$. In other words, as long as radius of the reflecting surface falls into the range above, the detector cannot receive the infrared flux emitted by the external thermal background through the reflection of the spherical reflecting surface. As shown in Fig. 2, $D(x_D, y_D)$ is on the reflecting surface to prevent the external thermal background radiation from reaching the detector directly. The outline radius of a concave mirror in the *oy* axis must be larger than y_D. Besides, the diameter of the spherical reflecting surface limits the maximum outline diameter. In conclusion, the outline diameter of the concave mirror should be limited to $D_0 \in [2y_D, 2R]$.

B. Design of the Neutral-Density Filter

According to the analysis in Section 2, the absorption-type filter cannot stop the radiant energy from reaching the detector effectively, providing that the incident flux is emitted by a reference at ambient temperature. Additionally, reflection-type filters have similar disadvantages, although the self-radiation is extraordinary low. The stray radiation is primarily introduced by reflecting the ambient radiation out of the Dewar. This paper proposes that if the neutral-density filter with a concave mirror is reasonably designed, the stray radiation introduced can be effectively suppressed. First, by theoretical analysis and ray tracing, it can be seen that the external ambient radiation cannot reach the detector by reflecting when the neutral-density filter is close to the cold shield of the detector and its clear aperture is quite small. By designing the dimension and mounting position of the filter and the concave mirror properly, the external radiation can be prevented from reaching the detector by reflection. Figure 3 shows the design method of a neutral-density filter.

Suppose the diameter of the filter is d'; the radiation emitted by point C, outside the cold shield, at ambient temperature is reflected from point B' (on the filter) to point A (on the detector); hence stray radiation is introduced. If the diameter of the filter is reduced to d, reverse ray tracing from point A of the detector results in a reflection point B and an emission point C, which is at the edge of the cold shield; hence no stray radiation is introduced. The ray path CBA determines the maximum diameter of the filter that does not introduce external stray radiation. However, the filter does not completely cover the entrance angle of the detector that is determined by the cold shield, so it is necessary to add a concave mirror with a center hole to mount the filter. The function of the concave mirror is to block the light outside the filter. It shall be properly designed according to the method proposed above to reduce the stray radiation introduced.

As shown in Fig. 3, S_f is the distance between the detector and the neutral-density filter. It should be noted that, in order to simplify the model, the thicknesses of the filter and the concave mirror are ignored. The distance between the vertex of the concave mirror and the detector is denoted by S_{cm}. Then we obtain

$$S_f = S_{cm} - \left(R - \sqrt{R^2 - d_m^2/4}\right). \tag{13}$$

The maximum diameter of the neutral-density filter is determined by the critical ray path CBA. The incident and exit angle of point B is expressed by θ. According to geometric principle,

$$(S_f - S_{cs}) \cdot \tan\theta = D_{cs}/2 - (S_f \cdot \tan\theta - D_{det}/2). \tag{14}$$

The maximum allowable diameter d_m of the filter can be expressed as a function of θ,

$$d_m = 2 \cdot S_f \cdot \tan\theta - D_{det}. \tag{15}$$

By solving Eqs. (12)–(15), d_m can be calculated by

$$d_m = \frac{S_f}{2S_f - S_{cs}} \cdot D_{cs} + \frac{S_{cs} - S_f}{2S_f - S_{cs}} \cdot D_{det}. \tag{16}$$

The formulas above indicate that, given the distance between the filter and the detector S_f, the external ambient radiation cannot reach the detector as long as the diameter d of the filter

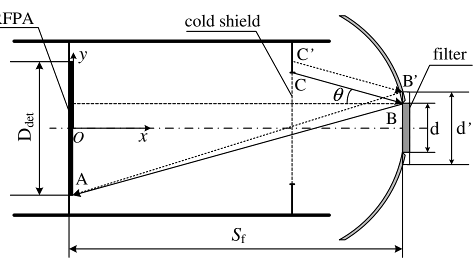

Fig. 3. Design method of a neutral-density filter that introduces low stray radiation.

is less than d_m. The ring between diameter d_m and d shall be coated by film with high reflectivity. It is worth noting that the F number of an infrared imager having such filter is naturally smaller than that determined by the cold shield. Therefore, it should be ensured that the F number of the designed optical system is almost equal to the F number defined by the neutral-density filter, instead of that defined by the cold shield.

By using the above-described filter in combination with a concave mirror, the incident radiation can be effectively attenuated while introducing extremely low stray radiation. Furthermore, the advantage of the filter designed above is more significant when the incident reference is at or close to ambient temperature. The concave mirrors and neutral-density filters are designed according to the method proposed in this paper. Two neutral-density filters with 100% and 50% transmittance are used to attenuate the incident flux by 0% and 50%, respectively. If the incident radiation is generated by a target at ambient temperature, 100% transmittance is a "high-temperature point" while 50% transmittance refers to a "low-temperature point." The two points obtained by using neutral-density filters are regarded, respectively, as a high-temperature target and a low-temperature target, which can be used for two-point NUC. By this method, we can perform two-point NUC by using a single reference at ambient temperature. The required single reference can be offered by a uniform lens cap, the clear sky, or other radiation sources. The proposed method, in principle, yields equivalent performance to conventional two-point NUC methods based on blackbody. Moreover, the correction reference is easy to obtain and the correction itself is easy to operate. So it is obviously superior to the conventional blackbody-based two-point NUC methods in convenience and cost.

4. ANALYSIS AND EXPERIMENTAL RESULTS

A. Neutral-Density Filter Design, Simulation, and Fabrication

To further evaluate the performance of the proposed two-point NUC method experimentally, a neutral-density filter and a concave mirror are designed and fabricated. They are designed for an F#2 mid-wave infrared imager with a cooled detector. Key parameters of the detector are shown in Table 1.

D_{det}, the diagonal length of the IRFPA, is 12.29 mm according to Table 1. Considering the convenience and security of practical application, we set the distance between the filter and the cold shield to 7 mm. So the distance S_f is 27 mm. Submitting the values mentioned above to Eq. (16), we obtain $d_m = 5.4$ mm. In other words, the diameter of the filter shall

Table 1. Parameters of the Detector

F number	2
Wave range/μm	3.7–4.8
Dynamic range/bit	14
pixel number	640 × 512
Pixel size/μm	15
IRFPA dimension/mm	9.60 × 7.68
Diameter of the cold shield/mm	10
Distance between cold shield and detector/mm	20
Temperature of the detector/K	77
NETD/mK	25 at 20°C

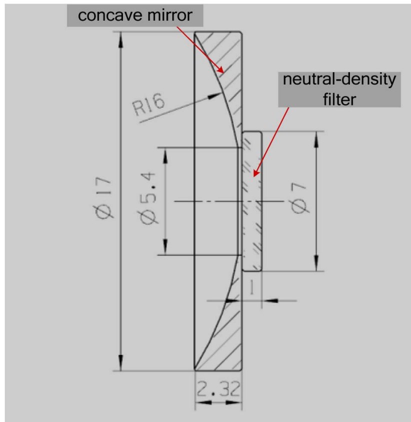

Fig. 4. Dimensions of the neutral-density filter and the concave mirror.

be smaller than 5.4 mm; hence the possible F number ranges from 5.0 to infinite. The diameter of the filter is determined by the F number that is required. By submitting the parameters above to Eqs. (5)–(12) and solving these equations, we get the range of radius $R \in [10.9, 17.2]$. We set R to 16 mm and continue the calculation. The distance between the vertex—top of the reflecting concave surface—and the detector is calculated by Eq. (13), $S_{cm} = 27.2$ mm. Submitting Eq. (6) to Eq. (5), we get the minimum diameter of the concave mirror, which equals 15.8 mm. Furthermore, the diameter D_0 ranges from 15.8 mm to 32 mm. We set the diameter to 17 mm.

The filter and the concave mirror are designed and analyzed before manufacture. Figure 4 shows one of the mechanical drawings. Note that the coated surface of the filter is recommended to be as close as possible to the detector in order to match the calculation model.

To verify whether the design is correct, and further to estimate the tolerances of installation and manufacture, we set up a model in TracePro to conduct ray tracing. If no light can reach the detector via reflection of the neutral-density filter or the concave mirror, the design results are proved to be reasonable. Figure 5 shows the model in TracePro. The IRFPA detector, the Dewar, the cold shield, the filter, and the concave mirror are identical to Fig. 4 in dimensions. To simplify the analysis, the outside ambient background is simulated by a ring near the cold shield. Moreover, the scattered rays inside the

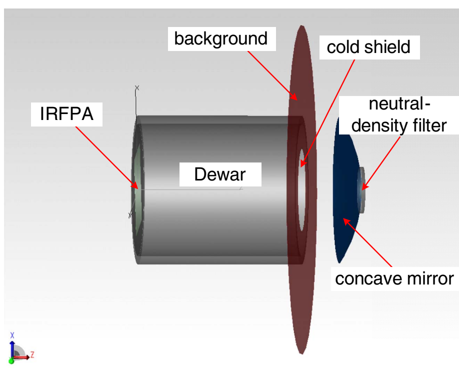

Fig. 5. Model of the filter and the detector in TracePro.

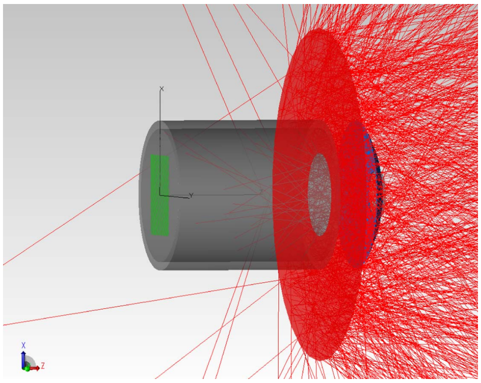

Fig. 6. Traced rays originated from ambient radiation in TracePro.

Dewar are ignored by setting the Dewar as a perfect absorber. The transmittance of the neutral-density filter is set to 100% and 50%, respectively, for ray tracing. The model in TracePro and the rays are shown in Figs. 5 and 6.

One billion rays are traced, and the irradiance/illuminance map output by TracePro illustrates that no ray reaches the IRFPA by reflection of the filter or the concave mirror. Hence the design proposed above is reasonable.

The material of the concave mirror can be selected from glass, plastic, or metal. Accordingly, a variety of machining methods can be used, such as die casting, polishing, and diamond turning. Coating of the reflecting surface can be selected according to the cost constraints and performance requirements of imaging. For general applications, aluminum film with about 90% reflectivity can be used for surface coating, whereas better performance requires gold film or even dielectric films whose reflectivity reaches almost 99% to minimize the radiation emitted by the coated reflecting surface. On the basis of practicality and cost considerations, the concave mirror is made of glass, while the reflecting surface is polished and coated with aluminum in this paper. The average reflectivity is about 90% across the spectral band from 3.7 μm to 4.8 μm; the emissivity is therefore about 10%. The neutral-density filters are coated to achieve 100% and 50% transmittance, respectively. Given that 100% transmittance is impossible, the two filters in reality have about 95% and 50% transmittance, respectively.

B. Nonuniformity Correction of an Infrared Image

To verify the performance of the proposed NUC method in this paper, NUCs were carried out for the image of a scene with targets at different temperatures. Three kinds of NUC techniques are conducted, namely one-point NUC, two-point NUC, and the proposed method. A lens cap at ambient temperature is used as the reference. First the 100% transmittance filter with a concave mirror is inserted to collect 20 images at "high temperature." Then we switch to the 50% filter to obtain 20 images at "low temperature." Afterwards, neutral-density filter based two-point NUC can be performed.

Figure 7 shows a raw image obtained by an infrared imaging system. The dark areas are targets at about ambient temperature, and the brighter square area is a uniform radiator at about 50°C. Obviously, there are lots of stripes and bright/dark spots in the image.

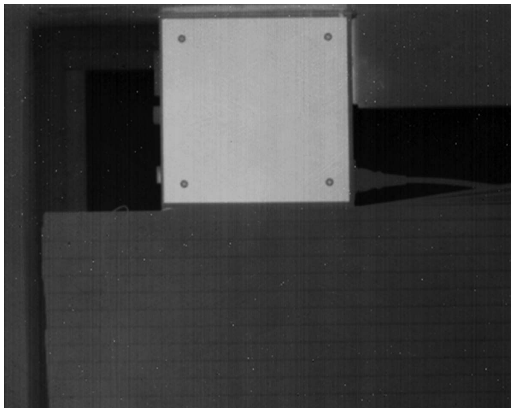

Fig. 7. Raw image in poor quality.

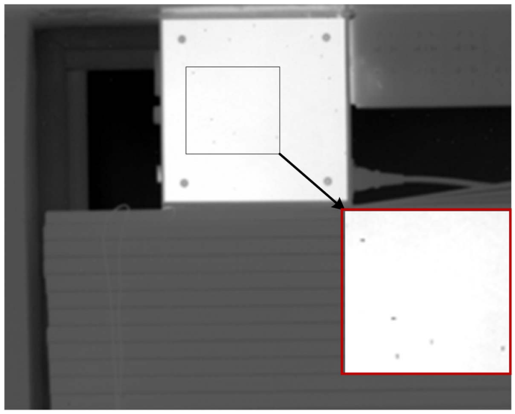

Fig. 8. Image corrected by one-point NUC.

First, one-point NUC was conducted using a painted black lens cap at ambient temperature. The image after one-point NUC is shown in Fig. 8; it is obvious that the performance of one-point NUC is favorable for the background area with targets at about ambient temperature. However, there are some black spots in the bright area (target at 50°C), which is illustrated in the drawing of partial enlargement. Hence the performance of one-point NUC is not good enough for infrared imaging.

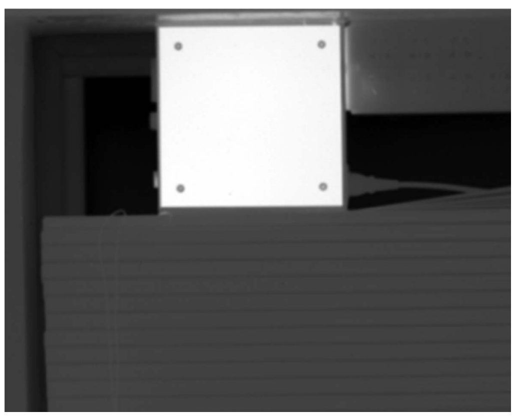

Fig. 9. Image corrected by conventional two-point NUC.

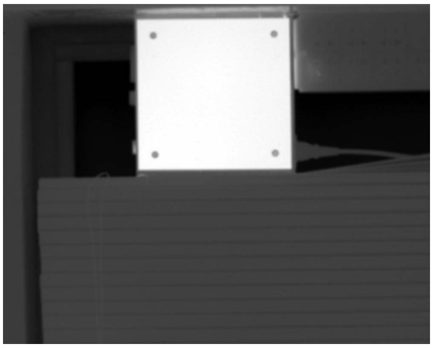

Fig. 10. Image corrected by the proposed two-point NUC.

The performance of conventional two-point NUC is shown in Fig. 9. The correction results of both the high-temperature and low-temperature targets are satisfactory, and there are no obvious spots or stripes.

As shown in Fig. 10, the proposed method can remove the stripes and spots of the raw image effectively, and the correction performance of high- and low-temperature targets is almost equivalent to Fig. 10. In conclusion, the proposed method can effectively realize NUC for targets at different temperatures, and the performance is comparable with that of the conventional two-point NUC.

C. Experiments to Evaluate the Proposed NUC Method Quantitatively

To further evaluate the proposed NUC method quantitatively, we used an MWIR camera for imaging and NUC, as shown in Fig. 11. The extended-area blackbody, selected as the reference source and the scene for imaging, has a 300 mm × 300 mm size and exhibits high effective emissivity (0.97 in the 3.7–4.8 μm waveband). Its temperature accuracy is about ±0.02°C over an operating temperature range of 0–150°C. Besides, a lens cap with uniform black paint is used as another reference source to test the performance of the proposed NUC method.

In order to evaluate the nonuniformity of the IRPFA quantitatively, a number of nonuniformity evaluation indicators have been proposed using uniform blackbody radiation. At present, the most commonly used one is NU, which can be expressed as [12,13]

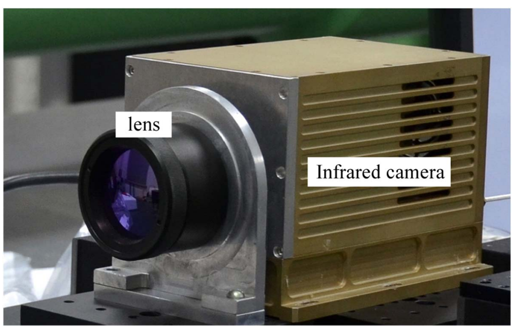

Fig. 11. Mid-wave infrared camera with lens and cooled detector.

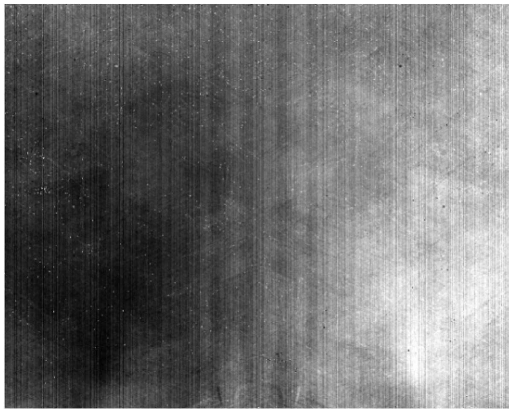

Fig. 12. Raw image of a blackbody at ambient temperature.

$$\mathrm{NU} = \frac{1}{\overline{Y}} \sqrt{\frac{1}{M \times N} \sum_{i=1}^{M} \sum_{j=1}^{N} (Y_{i,j} - \overline{Y})^2} \times 100\%, \tag{17}$$

where $Y_{i,j}$ is the gray value of pixel (i, j) in the corrected image, and $\overline{Y}$ denotes the average value of all pixels. The image of the blackbody at ambient temperature, 24.1°C, is shown in Fig. 12. The NU of the raw image is 5.45%, which is unacceptable for infrared imaging. In addition, the image shows obvious nonuniformity characterized by stripes, dark spots, bright spots, and bright areas. It is therefore necessary to perform NUC for the infrared imaging system.

The blackbody is set to 20°C, 25°C, …, 55°C, and the NUC performances of scenes at these temperatures are calculated according Eq. (17) to evaluate the NUC methods in detail. Two correction sources, namely a blackbody at ambient temperature and a uniform lens cap, are utilized to conduct one-point NUC, respectively. The conventional two-point NUC method uses the blackbody at 30°C and 20°C as the high- and low-temperature references, respectively. The proposed NUC method adopts the designed concave mirror and filters with 100% and 50% transmittance. The blackbody at ambient temperature, as a standard radiation source, was used to evaluate the optimal performance of the proposed NUC method. Additionally, a lens cap, which is easy to obtain, is employed as another reference for comparison.

Images of the blackbody at various temperatures are corrected by one-point NUC, two-point NUC, and the proposed method. As shown in Fig. 13, the temperatures of the scenes vary from 20°C to 55°C, with 5°C as the interval. The average NU of raw images is 3.72%, which is unacceptable for imaging or radiometry applications. (1) References at 30°C and 20°C are used as the high- and low-temperature references, respectively, to conduct the conventional two-point NUC. After correction, the average NUs of scenes at different temperatures varying from 20°C to 55°C were decreased to 0.25%, or 6.7% of the raw NU. So the performance of two-point NUC is quite satisfactory. Given that two-point NUC has the ability to correct gains and offsets of pixels perfectly, the slightly increased NUs according to scene temperatures mainly result from the shot noise and nonlinear response of the detectors. (2) One-point NUC is performed using a blackbody at ambient

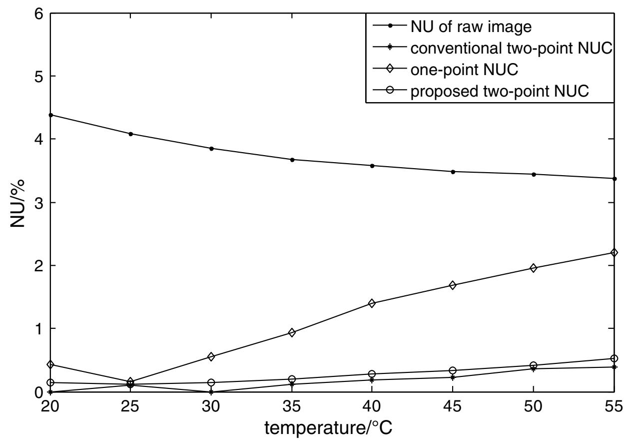

Fig. 13. Performance of NUC methods versus reference temperatures.

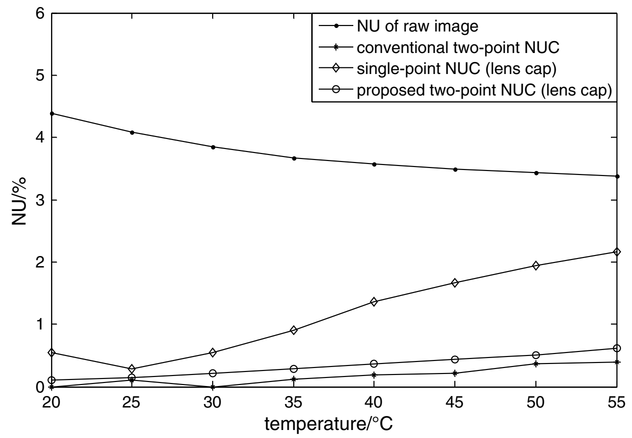

Fig. 14. Performance of NUC methods using a lens cap.

temperature, namely 24.1°C. Figure 13 shows that the performance of NUC is better when the scene temperature is closer to ambient temperature. In detail, the residual NU of corrected images at 25°C is 0.15%, which is excellent for infrared imaging, whereas the NU of raw images at 55°C is 3.40% and decreases to 2.21% after one-point NUC. 2.21% is naturally a bad performance for infrared imaging. In a word, one-point NUC is not a good choice for NUC of high-end infrared imagers. Experimental results of one-point NUC are in agreement with the theoretical analysis in the previous sections. (3) The proposed method, referring to neutral-density filter based two-point NUC, was carried out using a blackbody at ambient temperature, namely 24.1°C, as the single reference scene. Figure 12 and calculations demonstrate that the average NU of corrected images is 0.27%, which is almost equivalent to the conventional two-point calibration method.

For some low-cost infrared systems, it is not economical to equip a blackbody, which is quite expensive, only for NUC. Moreover, the working environments of infrared systems may be complicated; thereupon NUC is sometimes required to be conducted frequently to remove the effect of ambient temperature and internal heating. As a result, blackbody-based NUC may be not so practicable. Fortunately, almost all optical systems are equipped with a lens cap, which can be used as a substitute for blackbody. In this paper, a black-coated lens cap is used as a uniform reference for one-point NUC and the proposed two-point NUC methods; the results are shown in Fig. 14. The performance of one-point NUC using a lens cap is similar to that of the blackbody-reference-based method. The average NU of scenes corrected by the lens-cap-based two-point NUC method at 20°C to 55°C is 0.33%. The performance is a little worse than that of the blackbody-reference-based method mentioned above owing to nonuniformity of the lens cap, which is naturally not as good as a blackbody. However, the performance of lens-cap-based two-point NUC is good enough for infrared imaging, and it is significantly better than the one-point NUC. It is worth noting that the correction performance does not deteriorate significantly when the scene temperature changes. The performance of this method is slightly worse than blackbody-based two-point NUC because of the radiation nonuniformity of the lens cap. It is determined by the nonuniformity of surface emissivity and temperature. The uniformity of surface emissivity can be improved by black coating. Additionally, by using a metal lens cap with good thermal conductivity and performing NUC in a few seconds, we can improve the temperature uniformity effectively. So a lens cap is acceptable for conducting the proposed two-point NUC method.

Based on analysis of the correction performance of uniform scenes as well as an actual imaging scene, the proposed method has excellent adaptability and the performance is close to that of conventional two-point correction. The concave mirror is worth about \$200, the filter is worth about \$100, while the blackbody source is worth more than \$10,000. So NUC methods without using blackbodies are more economical. The lens-cap-based NUC method performs well and has minimal impact on temperature or radiance measurement accuracy. In general, It is an economical and convenient two-point correction method, which is suitable for various commercial and military infrared imaging systems.

5. CONCLUSION

This paper introduces a novel two-point NUC method based on specially designed neutral-density filters. It achieves two-point NUC with only one accessible reference, such as a lens cap at ambient temperature. The design method of the neutral-density filter with a concave mirror is explained in detail, and then simulated by ray tracing. Simulation results indicate that the filter has the ability to attenuate the incident radiation, while introducing extremely low stray radiation. For verification, a practical image of a complicated scene was corrected by several different NUC methods. It is demonstrated that the proposed method can effectively realize NUC for targets at different temperatures, and the performance is comparable with that of the conventional two-point NUC. In addition, uniform scenes are corrected using several NUC methods to further evaluate the proposed NUC method quantitatively. Experimental results show that the proposed two-point NUC, using a blackbody reference or a lens cap, yields almost equivalent performance to the conventional two-point NUC method.

The main advantages of the approach developed in this paper are listed as follows: (1) it yields almost the same performance compared to conventional two-point NUC; (2) it does not require expensive references, such as the blackbody, thus saving cost and benefitting the operator; (3) it improves the efficiency of two-point NUC, so the NUC coefficients can be updated more frequently.

REFERENCES

1. D. Zhou, D. Wang, L. Huo, R. Liu, and P. Jia, "Scene-based nonuniformity correction for airborne point target detection systems," Opt. Express **25**, 14210–14226 (2017).
2. B. Gutschwager and J. Hollandt, "Nonuniformity correction of imaging systems with a spatially nonhomogeneous radiation source," Appl. Opt. **54**, 10599–10605 (2015).
3. A. Rogalski, "Infrared detectors: an overview," Infrared Phys. Technol. **43**, 187–210 (2002).
4. Y. Cao and C. Tisse, "Single-image-based solution for optics temperature-dependent nonuniformity correction in an uncooled long-wave infrared camera," Opt. Lett. **39**, 646–648 (2014).
5. Z. He, Y. Cao, Y. Dong, J. Yang, Y. Cao, and C. Tisse, "Single-image-based nonuniformity correction of uncooled long-wave infrared detectors: a deep learning approach," Appl. Opt. **57**, D155–D164 (2018).
6. F. Marcotte, P. Tremblay, and V. Farley, "Infrared camera NUC calibration: comparison of advanced methods," Proc. SPIE **8706**, 870603 (2014).
7. Y. Jin, J. Jiang, and G. Zhang, "Three-step nonuniformity correction for a highly dynamic intensified charge-coupled device star sensor," Opt. Commun. **285**, 1753–1758 (2012).
8. M. Ochs, A. Schulz, and H.-J. Bauer, "High dynamic range infrared thermography by pixelwise radiometric self calibration," Infrared Phys. Technol. **53**, 112–119 (2010).
9. T. Svensson and I. Renhorn, "Evaluation of a method to radiometric calibrate hot target image data by using simple reference sources close to ambient temperature," Proc. SPIE **7662**, 76620X (2010).
10. W. L. Wolfe, *Introduction to Radiometry* (SPIE, 1998).
11. G. C. Holst, *Testing and Evaluation of Infrared Imaging Systems* (JCD, 1933).
12. L. Kun, C. Yang, P. Li, and Z. Bo, "Nonuniformity correction based on focal plane array temperature in uncooled long-wave infrared cameras without a shutter," Appl. Opt. **56**, 884–889 (2017).
13. X. Sui, Q. Chen, and G. Gu, "A novel non-uniformity evaluation metric of infrared imaging system," Infrared Phys. Technol. **60**, 155–160 (2013).